

Research Article

Aeromagnetic Compensation Algorithm Based on Principal Component Analysis

Peilin Wu ^{1,2}, Qunying Zhang,¹ Luzhao Chen ^{1,2}, Wanhua Zhu,¹ and Guangyou Fang¹

¹Key Laboratory of Electromagnetic Radiation and Sensing Technology, Institute of Electronics, Chinese Academy of Sciences, Beijing 100190, China

²University of Chinese Academy of Sciences, Beijing 100049, China

Correspondence should be addressed to Peilin Wu; wuwl924@foxmail.com

Received 26 May 2017; Revised 19 December 2017; Accepted 4 January 2018; Published 8 April 2018

Academic Editor: Jesus Corres

Copyright © 2018 Peilin Wu et al. This is an open access article distributed under the Creative Commons Attribution License, which permits unrestricted use, distribution, and reproduction in any medium, provided the original work is properly cited.

Aeromagnetic exploration is an important exploration method in geophysics. The data is typically measured by optically pumped magnetometer mounted on an aircraft. But any aircraft produces significant levels of magnetic interference. Therefore, aeromagnetic compensation is important in aeromagnetic exploration. However, multicollinearity of the aeromagnetic compensation model degrades the performance of the compensation. To address this issue, a novel aeromagnetic compensation method based on principal component analysis is proposed. Using the algorithm, the correlation in the feature matrix is eliminated and the principal components are used to construct the hyperplane to compensate the platform-generated magnetic fields. The algorithm was tested using a helicopter, and the obtained improvement ratio is 9.86. The compensated quality is almost the same or slightly better than the ridge regression. The validity of the proposed method was experimentally demonstrated.

1. Introduction

Aeromagnetic exploration is one of the most important exploration methods used in geophysical exploration, especially in mineral exploitations and underground unexploded ordnance detections [1–3]. Compared with surface magnetic survey, aeromagnetic exploration is a high efficiency and security method. Prospectors can finish a large survey area in a short time without any risk from the dangerous areas. Besides, the data measured by optically pumped magnetometer (OPM) is typically reliable and accurate [4].

The platform for aeromagnetic exploration is an aircraft like helicopter. Considering that the construction materials always contain some ferromagnetic materials, aircrafts can generate magnetic interference fields. The platform-generated fields degrade the measurement accuracy of the OPM, and this has necessitated the application of aeromagnetic compensation.

Aeromagnetic researches can trace back to World War II. In order to detect the submarine under water, U.S. researchers developed an aeromagnetic system. After the

war, because of its excellent application in geophysics, aeromagnetic was widely used in the civilian field. Meantime, aeromagnetic compensation methods were widely researched. The specific compensation model was proposed by Tolles in the 1940s [5]. He also designed a hardware compensation system [6]. After that, various compensation methods and systems were presented [7–13]. For instance, Leliak proposed sinusoidal maneuvers for compensating the platform-generated fields [14]. Leach proposed a ridge regression algorithm to solve multicollinearity in the aeromagnetic compensation model [15]. Leach's method can obtain good results in aeromagnetic compensation. But the method needs to calculate an optimal ridge coefficient. Sometimes it is difficult to calculate this optimal ridge coefficient.

To address multicollinearity in the model, we propose a novel method based on principal component analysis (PCA) to compensate platform-generated fields. This method uses an orthogonal transformation to convert a set of observations of possibly correlated variables into a set of values of linearly uncorrelated variables [16, 17]. After transformation, multicollinearity of the model is eliminated, and thus

least squares (LS) algorithm becomes more accurate. Compared with the ridge regression algorithm, the proposed method has almost the same or slightly better performance. Meanwhile, the proposed method is not necessary to calculate the optimal ridge coefficient and this makes it easier to be used in practice.

2. Aeromagnetic Compensation Model

2.1. Mathematical Expression of Aeromagnetic Compensation Model. Aeromagnetic compensation involves the suppression of the platform-generated fields. In exploration, the magnetic fields are measured by OPM, and the attitude angles of the platform are measured by a vector magnetometer. The direction cosines of the attitude angles of the platform are calculated by the output of the vector magnetometer as follows:

$$\begin{aligned} u_1 = \cos X(t) &= \frac{T(t)}{\sqrt{T(t)^2 + L(t)^2 + V(t)^2}}, \\ u_2 = \cos Y(t) &= \frac{L(t)}{\sqrt{T(t)^2 + L(t)^2 + V(t)^2}}, \\ u_3 = \cos Z(t) &= \frac{V(t)}{\sqrt{T(t)^2 + L(t)^2 + V(t)^2}}, \end{aligned} \quad (1)$$

where u_1 , u_2 , and u_3 are, respectively, the direction cosines of the attitude angles of the platform, and $T(t)$, $L(t)$, and $V(t)$ are, respectively, the transverse, longitudinal, and vertical components of Earth's total magnetic field measured by the vector magnetometer.

In the aeromagnetic compensation model, the platform-generated fields can be grouped into three types: permanent, induced, and eddy-current magnetic fields. The permanent magnetic fields caused by the permanent magnetism of the ferromagnetic parts of the platform can be given by

$$H_{\text{PERM}}(t) = c_1 u_1 + c_2 u_2 + c_3 u_3 = A_1 c_1 + A_2 c_2 + A_3 c_3, \quad (2)$$

where c_i , $i = 1, \dots, 3$, denotes the compensation coefficients of the permanent magnetic fields and A_i , $i = 1, \dots, 3$, denotes the variables constituted by the direction cosines.

The induced magnetic fields created in paramagnetic parts by the Earth's magnetic field can be given by

$$\begin{aligned} H_{\text{IND}}(t) &= H_e(t)(c_4 u_1^2 + c_5 u_1 u_2 + c_6 u_1 u_3 + c_7 u_2^2 + c_8 u_2 u_3 + c_9 u_3^2) \\ &= A_4 c_4 + A_5 c_5 + A_6 c_6 + A_7 c_7 + A_8 c_8 + A_9 c_9, \end{aligned} \quad (3)$$

where $H_e(t)$ is the Earth's magnetic field which can be calculated by $\sqrt{T(t)^2 + L(t)^2 + V(t)^2}$; c_i , $i = 4, \dots, 9$, denotes the compensation coefficients of the induced magnetic fields; and A_i , $i = 4, \dots, 9$, denotes the variables consisting of the direction cosines and $H_e(t)$.

The eddy-current magnetic fields produced by eddy currents that occur in any electrical conducting path of the airframe can be given by

$$\begin{aligned} H_{\text{EDDY}}(t) &= H_e \left(c_{10} u_1 u_1' + c_{11} u_1 u_2' + c_{12} u_1 u_3' \right. \\ &\quad \left. + c_{13} u_2 u_1' + c_{14} u_2 u_2' + c_{15} u_2 u_3' \right. \\ &\quad \left. + c_{16} u_3 u_1' + c_{17} u_3 u_2' + c_{18} u_3 u_3' \right) \\ &= A_{10} c_{10} + A_{11} c_{11} + A_{12} c_{12} + A_{13} c_{13} + A_{14} c_{14} \\ &\quad + A_{15} c_{15} + A_{16} c_{16} + A_{17} c_{17} + A_{18} c_{18}, \end{aligned} \quad (4)$$

where u_1' , u_2' , and u_3' are, respectively, the time derivative of u_1 , u_2 , and u_3 ; c_i , $i = 10, \dots, 18$, denotes the compensation coefficients of the eddy-current magnetic fields; and A_i , $i = 10, \dots, 18$, denotes the variables consisting of the direction cosines and $H_e(t)$.

The platform-generated fields measured by OPM can be expressed as

$$H_d(t) = H_{\text{PERM}}(t) + H_{\text{IND}}(t) + H_{\text{EDDY}}(t) = \sum_{i=1}^{18} A_i c_i. \quad (5)$$

The corresponding matrix notations of (5) are expressed as

$$\mathbf{H}_d = \mathbf{A}\mathbf{C}, \quad (6)$$

where \mathbf{H}_d and \mathbf{C} are column vectors consisting of $H_d(t)$ and c_i , $i = 1, \dots, 18$; and \mathbf{A} is a feature matrix can be written as

$$\mathbf{A} = \begin{bmatrix} A_1(1) & A_2(1) & \cdots & A_{18}(1) \\ A_1(2) & A_2(2) & \cdots & A_{18}(2) \\ \vdots & \vdots & \ddots & \cdots \\ A_1(n) & A_2(n) & \cdots & A_{18}(n) \end{bmatrix}. \quad (7)$$

The LS algorithm is used to get an optimum solution of (6). It can be expressed as

$$\mathbf{C} = (\mathbf{A}^T \mathbf{A})^{-1} \mathbf{A}^T \mathbf{H}_d. \quad (8)$$

Because multicollinearity existed in the model, the inverse matrix of $\mathbf{A}^T \mathbf{A}$ does not exist; therefore, (8) cannot obtain the accurate compensation coefficients.

Considering the issue, by adding L_2 regularization term to the loss function of the LS algorithm, the new loss function can be given by

$$C_d = \|\mathbf{A}\mathbf{C} - \mathbf{H}_d\|^2 + \alpha \|\mathbf{C}\|^2, \quad (9)$$

where α is a ridge parameter. When α equals zero, (9) becomes the loss function of LS algorithm. By equating the partial derivative of (9) with respect to \mathbf{C} to zero, the expression can be given by

$$\frac{\partial C_d}{\partial \mathbf{C}} = 2\mathbf{A}^T (\mathbf{A}\mathbf{C} - \mathbf{H}_d) + 2\alpha \mathbf{C}. \quad (10)$$

The solution of (10) is

$$\mathbf{C} = (\mathbf{A}^T \mathbf{A} + \alpha \mathbf{I})^{-1} \mathbf{A}^T \mathbf{H}_d. \quad (11)$$

Compared with (8) in aeromagnetic compensation, (11) leads to better compensation results. In a typical case, using (11) in a calibration flight, the compensation coefficients can be obtained. Then by plugging the obtained compensation coefficients back into (6), the platform-generated fields can be fitted and compensated.

2.2. Multicollinearity of the Aeromagnetic Compensation Model and Assessment Criteria of Multicollinearity. Aeromagnetic compensation model is a linear model. In (6), multicollinearity exists between the variables $\mathbf{A}_1, \mathbf{A}_2, \dots, \mathbf{A}_{18}$, which are the column vectors of matrix \mathbf{A} . The relationship can be expressed as

$$\mathbf{A}_i = \sum_{j=1, j \neq i}^p b_j \mathbf{A}_j + c_0, \quad (12)$$

where parameters b_j are not all zeros and c_0 is a constant [18].

In (6), matrix \mathbf{A} is calculated by the different combinations of the direction cosines and its time derivative. Therefore, multicollinearity widely exists in the aeromagnetic compensation model. The typically multicollinearity relationships are derived from (3) and (4). They can be expressed as follows:

$$\begin{aligned} u_1^2 + u_2^2 + u_3^2 &= 1, \\ u_1 u_1' + u_2 u_2' + u_3 u_3' &= 0. \end{aligned} \quad (13)$$

Variance inflation factor (VIF) is used to quantify the severity of multicollinearity in the model [19]. First, the sum of squares of residuals can be expressed as follows:

$$\text{SSE}_i = \sum_{j=1}^n (\mathbf{A}_i(j) - \hat{\mathbf{A}}_i(j))^2, \quad (14)$$

where $\mathbf{A}_i(j)$ is the j th sampling point of the variable \mathbf{A}_i and $\hat{\mathbf{A}}_i(j)$ is the j th predicted value associated with $\mathbf{A}_i(j)$.

Then, the total sum of squares can be given by

$$\text{SST}_i = \sum_{j=1}^n (\mathbf{A}_i(j) - \bar{\mathbf{A}}_i(j))^2, \quad (15)$$

where $\bar{\mathbf{A}}_i(j)$ is the mean of the observed data.

After that, the coefficient of determination of the i th variable can be defined as

$$R_i^2 = 1 - \frac{\text{SSE}_i}{\text{SST}_i}. \quad (16)$$

From (16), the mathematical expression of VIF can be given by

$$\text{VIF}_i = (1 - R_i^2)^{-1}. \quad (17)$$

If the VIFs of the variables $\mathbf{A}_1, \mathbf{A}_2, \dots, \mathbf{A}_{18}$ of the calibration data are larger than 10, it means that multicollinearity is significant in the model. The LS algorithm cannot obtain accurate compensation results. Thus, PCA is introduced to eliminate multicollinearity in the model. After that, accurate compensation results are obtainable.

3. Aeromagnetic Compensation Method Based on PCA

PCA is a statistical procedure that uses an orthogonal transformation to convert a set of observations of possibly correlated variables into a set of values of linearly uncorrelated variables called principal components (PCs). Using appropriate PCs, the overlap of the useful information in matrix \mathbf{A} caused by multicollinearity can be addressed. Meantime, this method is effective to separate the noise and the useful information and improve the accuracy of aeromagnetic compensation.

In the aeromagnetic compensation model, the PCA extracts m PCs $\mathbf{F}_1, \mathbf{F}_2, \dots, \mathbf{F}_m$ from the variables $\mathbf{A}_1, \mathbf{A}_2, \dots, \mathbf{A}_{18}$, where $m \leq 18$. After PCA, the feature matrix \mathbf{A} is converted into a new feature matrix \mathbf{F} , which consists of column vectors \mathbf{F}_i . If there is no multicollinearity in the model, the matrix \mathbf{F} and \mathbf{A} have same number of columns; if multicollinearity exists, the number of columns of \mathbf{F} is less.

3.1. Process of the Method. The structure of the aeromagnetic compensation method based on PCA is shown in Figure 1.

The specific steps are as follows:

- (1) The feature vectors $\mathbf{A}_{1_cal}, \mathbf{A}_{2_cal}, \dots, \mathbf{A}_{18_cal}$ obtained by calibration flight data should be standardized as

$$\tilde{\mathbf{A}}_{i_cal} = \frac{\mathbf{A}_{i_cal} - \bar{\mathbf{A}}_{i_cal}}{s_{i_cal}}, \quad i = 1, \dots, 18, \quad (18)$$

where $\tilde{\mathbf{A}}_{i_cal}$ is the i th column vector of the standardized calibration flight matrix $\tilde{\mathbf{A}}_{cal}$; \mathbf{A}_{i_cal} is the i th column vector of the calibration flight matrix \mathbf{A}_{cal} ; $\bar{\mathbf{A}}_{i_cal}$ and s_{i_cal} are, respectively, the mean and standard deviation of the corresponding observed data.

- (2) Calculate the covariance matrix of the matrix $\tilde{\mathbf{A}}_{cal}$ and denote it as \mathbf{V} .
- (3) Calculate the 18 eigenvalues of the covariance matrix \mathbf{V} , and list them as $\lambda_1 \geq \lambda_2 \geq \dots \geq \lambda_{18}$. Then obtain the corresponding eigenvectors $\mathbf{a}_1, \mathbf{a}_2, \dots$, and \mathbf{a}_{18} .
- (4) The i th PC can be expressed as

$$\mathbf{F}_{i_cal} = \tilde{\mathbf{A}}_{cal} \mathbf{a}_i. \quad (19)$$

Then rank the PCs by their contributions. The new calibration flight matrix consisting of PCs can be denoted as $\mathbf{F}_{cal} = [\mathbf{F}_{1_cal} \ \mathbf{F}_{2_cal} \ \dots \ \mathbf{F}_{m_cal}]$, where $m \leq 18$. Thus, the relationship between $\tilde{\mathbf{A}}_{cal}$ and \mathbf{F}_{cal} can be given by

$$\mathbf{F}_{cal} = \tilde{\mathbf{A}}_{cal} \mathbf{a}, \quad (20)$$

where \mathbf{a} is the matrix consisting of the corresponding eigenvectors.

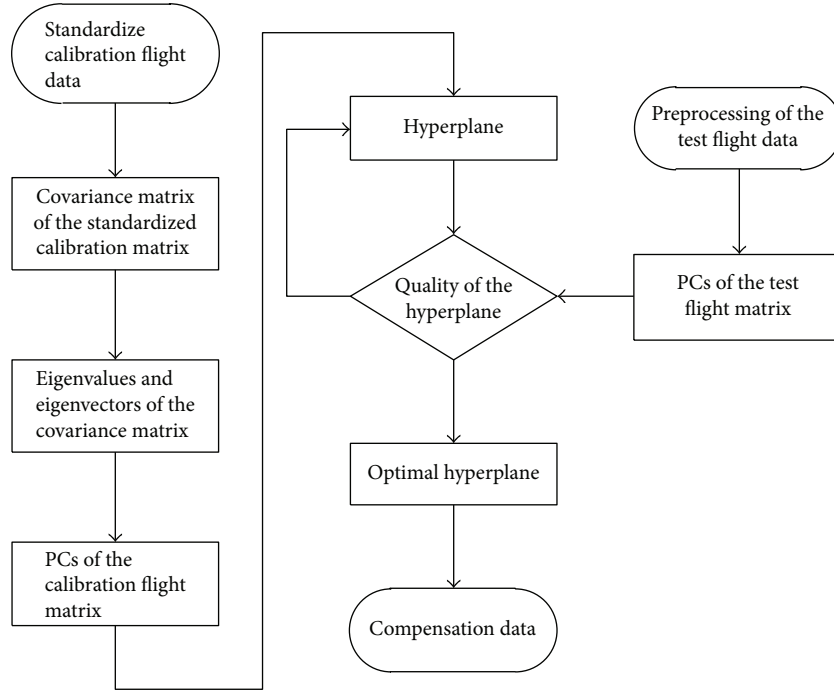


FIGURE 1: Structure of the algorithm.

Using the calibration flight data, the aeromagnetic compensation coefficients can be calculated by LS algorithm, which is expressed as

$$\mathbf{C}_{pca} = (\mathbf{F}_{cal}^T \mathbf{F}_{cal})^{-1} \mathbf{F}_{cal}^T \mathbf{H}_d. \quad (21)$$

- (5) Using the mean and standard deviation of the matrix \mathbf{A}_{cal} , the corresponding test flight matrix \mathbf{A}_{test} can be standardized as

$$\tilde{\mathbf{A}}_{i_test} = \frac{\mathbf{A}_{i_test} - \bar{\mathbf{A}}_{i_cal}}{s_{i_cal}}, i = 1, \dots, 18, \quad (22)$$

where $\tilde{\mathbf{A}}_{i_test}$ is the i th standardized column vectors consisting of the standardized test flight matrix $\tilde{\mathbf{A}}_{test}$ and \mathbf{A}_{i_test} is the i th column vectors consisting of the test flight matrix \mathbf{A}_{test} .

- (6) Calculate the new test flight matrix consisting of PCs from the standardized test flight matrix $\tilde{\mathbf{A}}_{test}$ as follows:

$$\mathbf{F}_{test} = \tilde{\mathbf{A}}_{test} \mathbf{a}, \quad (23)$$

where \mathbf{F}_{test} is the new test flight matrix. Then the compensation data can be obtained by

$$\mathbf{H}_{Comp_test} = \mathbf{H}_{OPM_test} - \mathbf{F}_{test} \mathbf{C}_{pca}, \quad (24)$$

where \mathbf{H}_{OPM_test} is the data measured by OPM before compensation; and \mathbf{H}_{Comp_test} is the data after compensation.

The optimal number of the the PCs is determined through assessing quality of the compensated data. Then the optimal compensation hyperplane is obtained.

3.2. Assessment Criteria for the Number of PCs. The key point in the proposed method is to choose the PCs. Too few PCs cannot compensate the platform-generated fields, while too many PCs cannot eliminate multicollinearity in the aeromagnetic compensation model. Therefore, it is necessary to choose appropriate number of PCs.

The test flight is used to address this issue. First, the PCs are ranked by their contributions to the model. Then in this order, the PCs enter the model in sequence. Meantime, the improvement ratios (IR) are assessed by [20]

$$IR = \frac{\sigma_u}{\sigma_c}, \quad (25)$$

where σ_u is the standard deviation of the uncompensated data; and σ_c is the standard deviation of the compensation data. If the IR obtains maximal value, the number of the PCs in the model is optimal.

4. Results and Discussion

4.1. Helicopter Experiment. A helicopter mounted with a straight rod was used to carry out an experiment to demonstrate the validity of the method. The helicopter and its experimental flight path are shown in Figure 2. The OPM is mounted at the front of the straight rod.

In order to avoid being disturbed by the magnetic interference of the ground, the experimental height was about 3000 m. First the helicopter flew a calibration box, and then

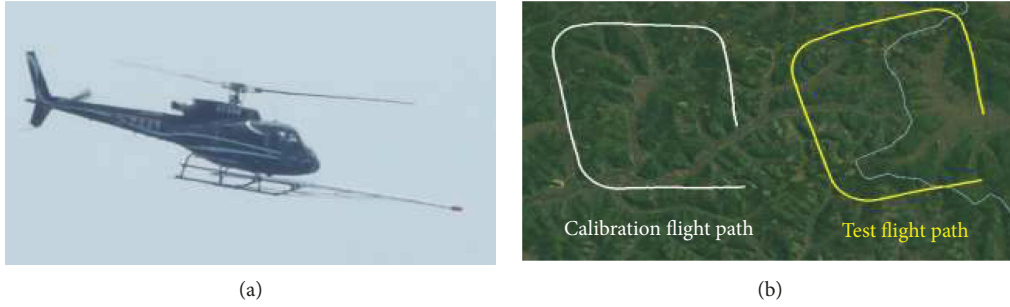


FIGURE 2: Helicopter and flight path: (a) helicopter mounted with straight rod and (b) calibration flight path and test flight path in Google earth.

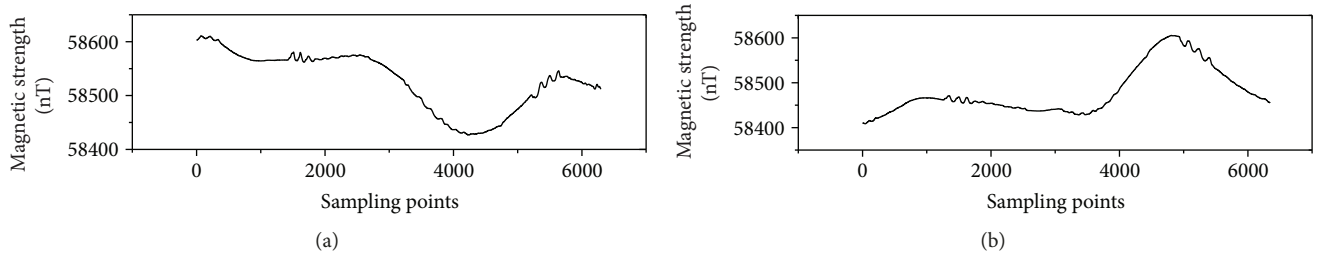


FIGURE 3: Magnetic fields measured by OPM: (a) calibration flight data and (b) test flight data.

a test box was flown. These two flight boxes are very similar. Both of them contain four orthogonal magnetic headings, and each line of the boxes contains calibration maneuvers consisting of $\pm 10^\circ$ rolls, $\pm 5^\circ$ pitches, and $\pm 5^\circ$ yaws. In ideal calibration flight, the calibration box and the test box are in the same shape. However, in practical flight, it is difficult to keep these two boxes in the same shape, for the impact of air-flow, operation accuracy of the pilot, and some other reasons like accuracy of flight control system. However, these unsatisfactory factors have little effect on the performance of aeromagnetic compensation. The calibration flight is used to obtain a compensation hyperplane, and the test flight is used to assess the performance of the compensation hyperplane. After the compensation hyperplane is assessed, the optimal number of the PCs is obtained. The original measurement data are shown in Figure 3.

4.2. Quantitative Analysis of the Experimental Results. The multicollinearity analysis is applied to the calibration flight data before compensation. The VIFs of the variables of the calibration flight data are listed in Table 1.

In Table 1, all VIFs of variables are greater than 10, and the phenomenon means that multicollinearity is obvious in the model. Using the method based on PCA, multicollinearity of the model is eliminated. And all VIFs of the new variables are equal to one.

The relationship between the IRs and the numbers of the PCs is shown in Figure 4. The vertical axis is the value of IR and the horizontal axis is the number of the PCs entering the model.

Figure 4(b) shows that the maximal IR is obtained when the number is 14. It means that the corresponding hyperplane is the optimal compensation hyperplane. Figure 5

TABLE 1: VIFs of variables.

Feature vector	VIF
A_1	8142.6
A_2	4695.3
A_3	157,858
A_4	692.8
A_5	119.8
A_6	3962.3
A_7	148.4
A_8	3049.2
A_9	20024.9
A_{10}	12508.5
A_{11}	17.2
A_{12}	51.2
A_{13}	24.7
A_{14}	16.5
A_{15}	25.5
A_{16}	73.9
A_{17}	41.5
A_{18}	218.1

shows the compensation results of the calibration and test flight data by using the optimal compensation hyperplane.

In Figure 5, the dash line is the uncompensated data, which is the original data processed by a filter. The uncompensated data corresponds to the left vertical axis. The solid line is the compensated data, which corresponds to the right vertical axis.

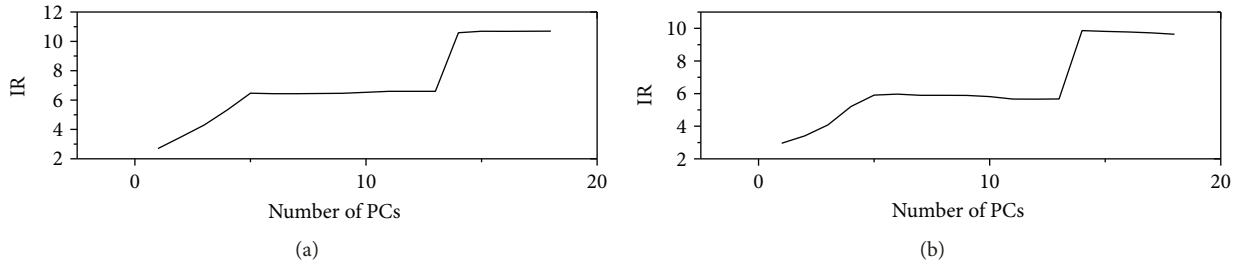


FIGURE 4: IR-PCs results: (a) calibration flight data and (b) test flight data.

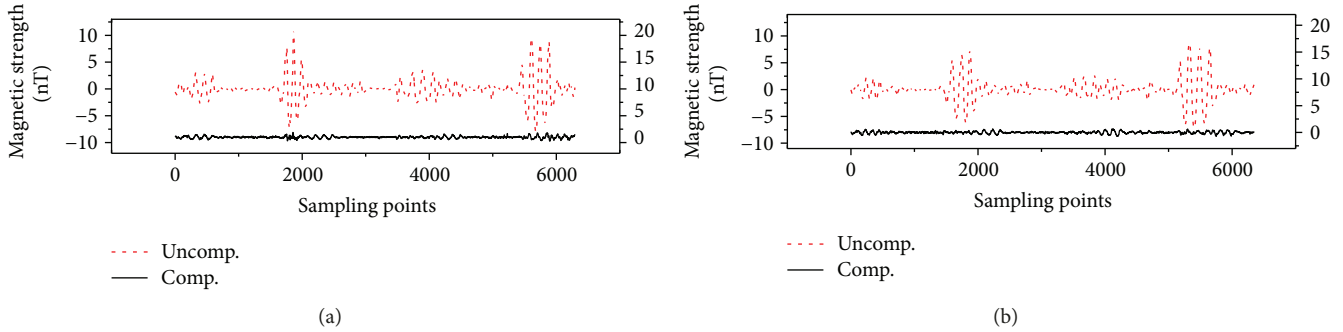


FIGURE 5: Aeromagnetic compensation by PCA-based method: (a) calibration flight data and (b) test flight data.

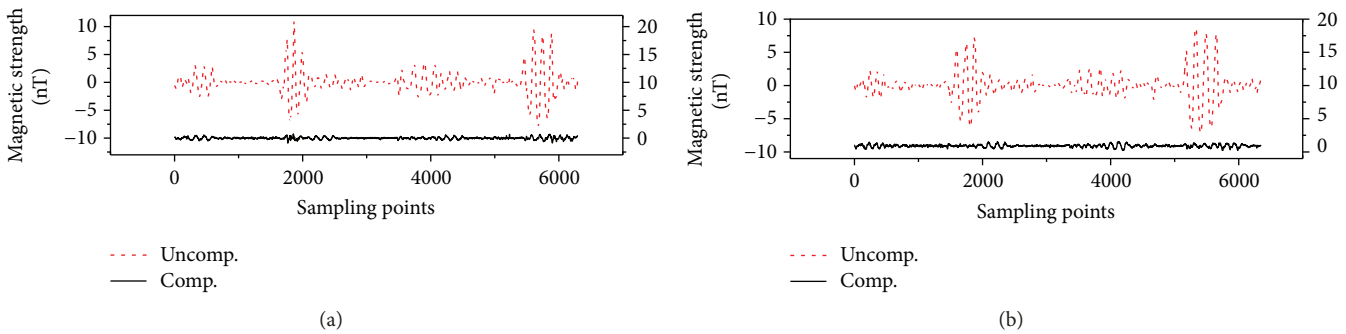


FIGURE 6: Aeromagnetic compensation by ridge regression-based method: (a) calibration flight data and (b) test flight data.

TABLE 2: Standard deviation and IR of different methods.

		Uncompensated	Compensated	IR
Ridge regression	Calibration flight	2.1106	0.1975	10.6875
	Test flight	2.0360	0.2074	9.8149
PCA	Calibration flight	2.1106	0.1993	10.5903
	Test flight	2.0360	0.2064	9.8642

Figure 5 shows that the method based on PCA can obtain good compensation results. Compared with the ridge regression results using the optimal ridge coefficient shown in Figure 6, the method based on PCA has almost the same compensation performance.

In Figure 6, the dash line is the uncompensated data, which corresponds to the left vertical axis. The solid line is the compensated data, which corresponds to the right vertical axis.

The standard deviation and IR are used to assess the results of the different methods. The quantitative comparisons of two methods are presented in Table 2.

Table 2 shows that both of these compensation methods can compensate OPM data well. The performance of the PCA-based method is almost the same or slightly better than the ridge regression method. Moreover, the PCA-based method is only needed to choose the number of PCs entering the model from 1 to 18, which is easier to realize in practice.

5. Conclusion

A novel PCA-based aeromagnetic compensation method is proposed in this paper. Through extracting the PCs of the feature matrix, multicollinearity in the model is

eliminated. The method enables effective removal of the platform-generated fields of the helicopter. The validity of the proposed method is experimentally demonstrated. The experimental results show that this method has the same or slightly better performance than the ridge regression method. Meanwhile, the method has no need to calculate an optimal ridge coefficient, and this simplifies the aeromagnetic compensation procedure.

Conflicts of Interest

The authors declare that they have no conflicts of interest.

Acknowledgments

This research is sponsored by R&D of Key Instruments and Technologies for Deep Resources Prospecting (the National R&D Projects for Key Scientific Instruments) of China under Grant no. ZDYZ2012-1-03.

References

- [1] M. N. Nabighian, V. J. S. Grauch, R. O. Hansen et al., "The historical development of the magnetic method in exploration," *Geophysics*, vol. 70, no. 6, pp. 33ND–61ND, 2005.
- [2] P. Hood, "History of aeromagnetic surveying in Canada," *The Leading Edge*, vol. 26, no. 11, pp. 1384–1392, 2007.
- [3] W. E. Doll, T. J. Gamey, D. T. Bell et al., "Historical development and performance of airborne magnetic and electromagnetic systems for mapping and detection of unexploded ordnance," *Journal of Environmental and Engineering Geophysics*, vol. 17, no. 1, pp. 1–17, 2012.
- [4] C. D. Hardwick, "Non-oriented cesium sensors for airborne magnetometry and gradiometry," *Geophysics*, vol. 49, no. 11, pp. 2024–2031, 1984.
- [5] W. E. Tolles, "Compensation of aircraft magnetic fields," US Patent 2692970 (1954).
- [6] W. E. Tolles, "Magnetic field compensation system," US Patent US2706801 (1955).
- [7] C. Guo, M. Ma, and D. Cheng, "A new solution of aircraft magnetic interference field based on errors-in-variables method," *Journal of Computational Intelligence and Electronic Systems*, vol. 4, no. 1, pp. 70–73, 2015.
- [8] B. Gu, Q. Li, and H. Liu, "Aeromagnetic compensation based on truncated singular value decomposition with an improved parameter-choice algorithm," in *2013 6th International Congress on Image and Signal Processing (CISP)*, pp. 1545–1551, Hangzhou, China, 2013.
- [9] B. Zhang, Z. Guo, and Y. Qiao, "A simplified aeromagnetic compensation model for low magnetism UAV platform," in *2011 IEEE International Geoscience and Remote Sensing Symposium*, pp. 3401–3404, Vancouver, BC, Canada, 2011.
- [10] Z. Dou, Q. Han, X. Niu, X. Peng, and H. Guo, "An aeromagnetic compensation coefficient-estimating method robust to geomagnetic gradient," *IEEE Geoscience and Remote Sensing Letters*, vol. 13, no. 5, pp. 611–615, 2016.
- [11] C. Lin, J.-J. Zhou, and Z.-Y. Yang, "A method to solve the aircraft magnetic field model basing on geomagnetic environment simulation," *Journal of Magnetism and Magnetic Materials*, vol. 384, pp. 314–319, 2015.
- [12] Y. Zou, X. Meng, L. Guo, X. Zhang, and C. Xiu, "Study on aeromagnetic full tensor compensation," in *International Workshop and Gravity, Electrical & Magnetic Methods and their Applications*, pp. 81–83, Chenghu, China, April 2015.
- [13] S. H. Bickel, "Small signal compensation of magnetic fields resulting from aircraft maneuvers," *IEEE Transactions on Aerospace and Electronic Systems*, vol. AES-15, no. 4, pp. 518–525, 1979.
- [14] P. Leliak, "Identification and evaluation of magnetic-field sources of magnetic airborne detector equipped aircraft," *IRE Transactions on Aeronautical and Navigational Electronics*, vol. ANE-8, no. 3, pp. 95–105, 1961.
- [15] B. W. Leach, "Aeromagnetic compensation as a linear regression problem," in *Information Linkage Between Applied Mathematics and Industry*, pp. 139–161, Academic Press, San Diego, CA, USA, 1980.
- [16] H. Abdi and L. J. Williams, "Principal component analysis," *Wiley Interdisciplinary Reviews: Computational Statistics*, vol. 2, no. 4, pp. 433–459, 2010.
- [17] J. Shlens, "A tutorial on principal component analysis," *OALib Journal*, vol. 51, no. 3, pp. 219–226, 2014.
- [18] A. Alin, "Multicollinearity," *Wiley Interdisciplinary Reviews: Computational Statistics*, vol. 2, no. 3, pp. 370–374, 2010.
- [19] L. M. Surhone, M. T. Tennoe, S. F. Henssonow, S. Deviation et al., *Variance Inflation Factor. Encyclopedia of Statistical Sciences*, John Wiley & Sons, Inc, New York City, NY, USA, 2004.
- [20] C. D. Hardwick, "Important design considerations for inboard airborne magnetic gradiometers," *Geophysics*, vol. 49, no. 11, pp. 2004–2018, 1984.



Hindawi

Submit your manuscripts at
www.hindawi.com

